

Supporting Information

Unravelling the Potential of Hybrid Borocarbonitride Biphenylene 2D Network for Thermoelectric Applications: A First Principles Study

Ajay Kumar^a Parbati Senapati^a and Prakash Parida^{a*}

^aDepartment of Physics, Indian Institute of Technology Patna, Bihta, Bihar, India, 801106

*Corresponding author: - pparida@iitp.ac.in

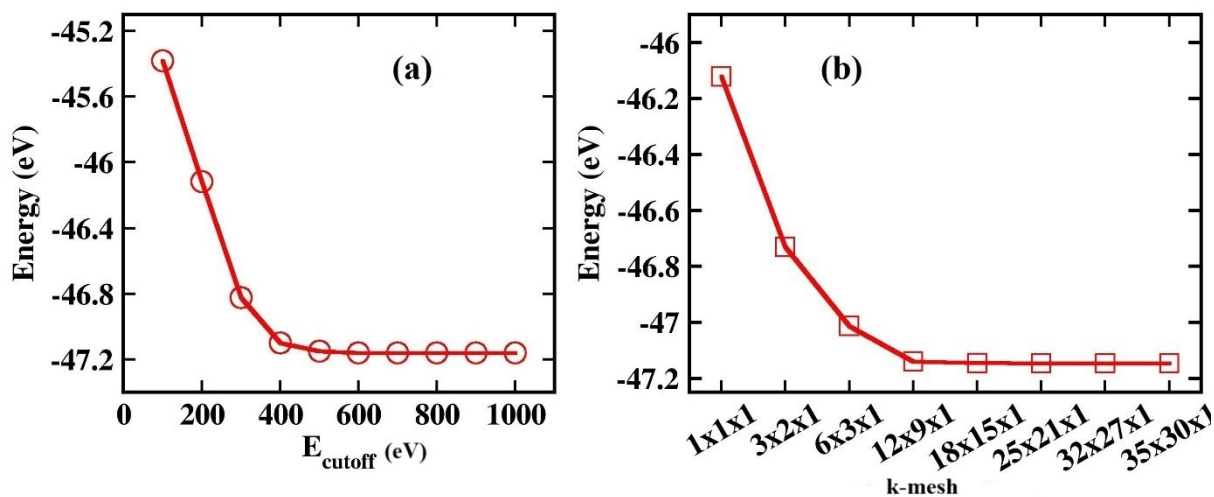


Fig. S1: Total energy versus plane wave energy cut off for plane wave and (b) the k-mesh plots for bpn-BCN monolayer.

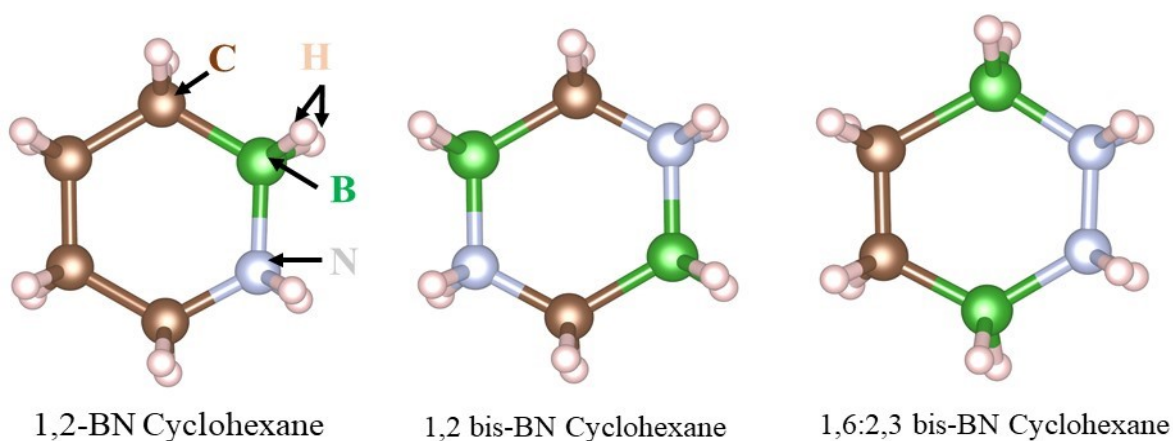


Fig. S2: Depicts the structures of precursors that can be use to synthesize the bpn-BCN monolayer.

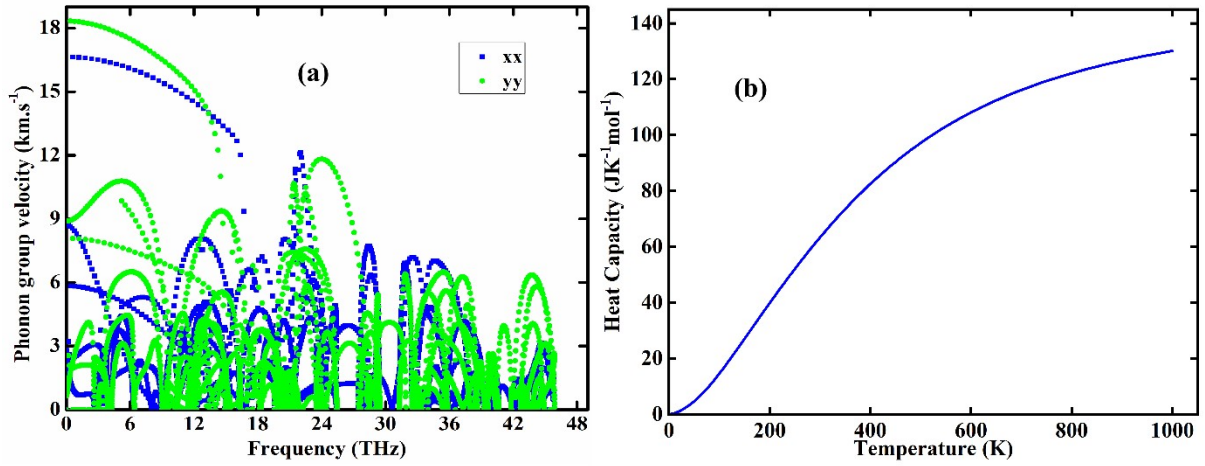


Fig. S3: (a) Anisotropic phonon group velocity versus frequency and (b) specific heat capacity at constant volume varies with temperature for bpn-BCN monolayer.

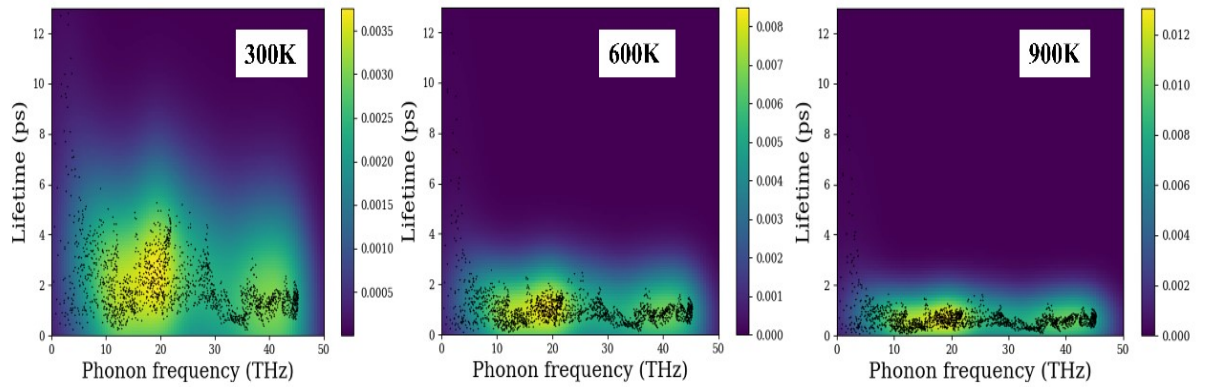


Fig. S4: Phonon lifetime versus phonon frequency at different temperatures (300K, 600K and 900K) in bpn-BCN monolayer.

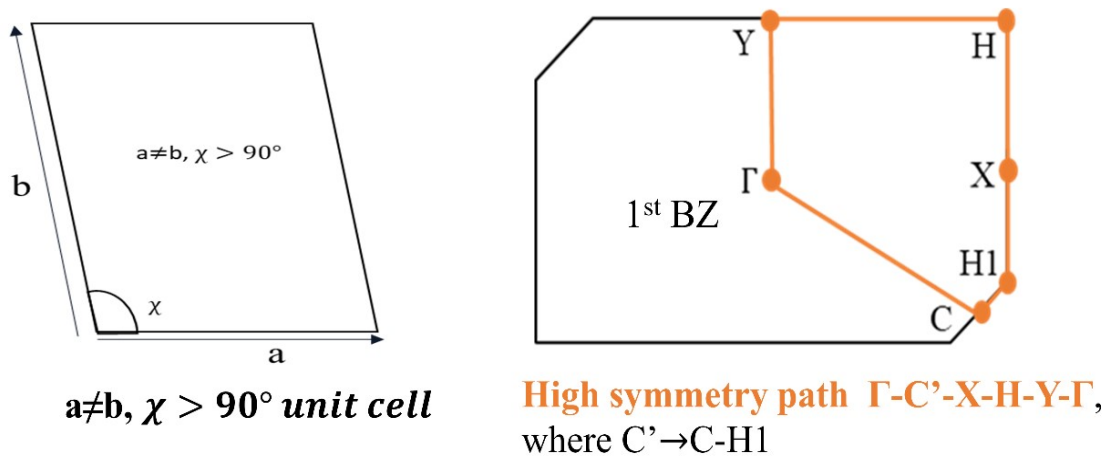


Fig. S5: Oblique unit cell and 1st Brillouin zone along with high symmetry point.

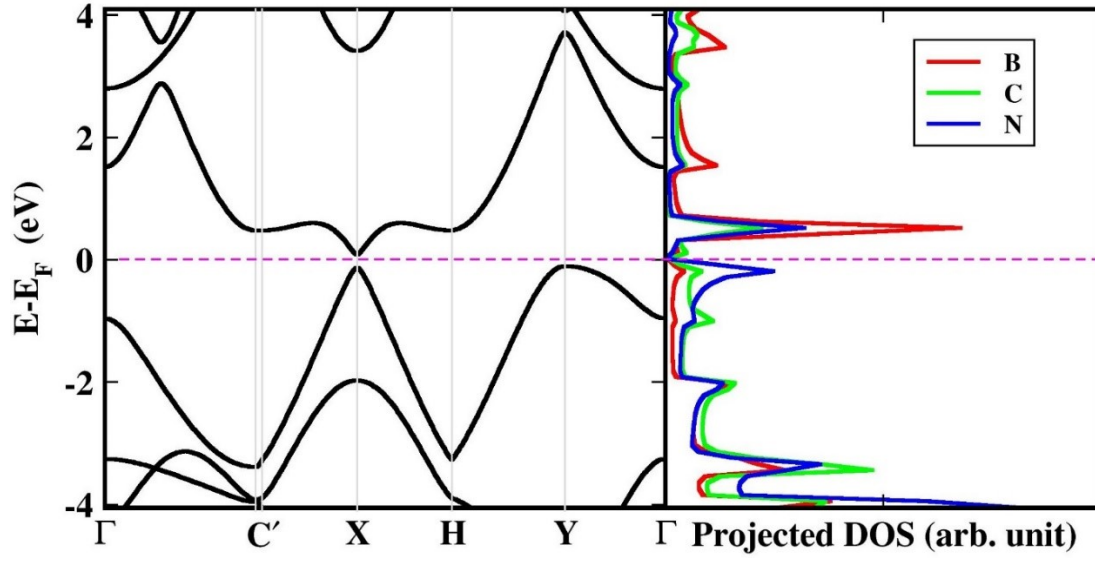


Fig. S6: Electronic band structure and projected density of states using GGA-PBE functional of bpn-BCN monolayer.

Table S1: The charge carrier, in-plane stiffness (C_{2D}), deformation potential constant (E_P) and carrier effective mass (m^*) in bpn-BCN have been calculated at a temperature of $T = 300$ K.

	Carrier	v_g (m/s)	C^{2D} (N/m)	E_P (eV)	$m^* (m_0)$	μ^{2D} ($cm^2V^{-1}s^{-1}$)	τ (fs)
bpn-BCN(x)	e	4.1×10^5	238.7	7.12	0.092	661.41	34.60
bpn-BCN(y)	e	4.1×10^5	217.8	10.36	0.058	497.16	16.39
bpn-BCN(x)	h	4.86×10^5	238.7	11.95	0.064	601.93	21.90
bpn-BCN(y)	h	4.86×10^5	217.8	7.01	0.041	707.90	16.50

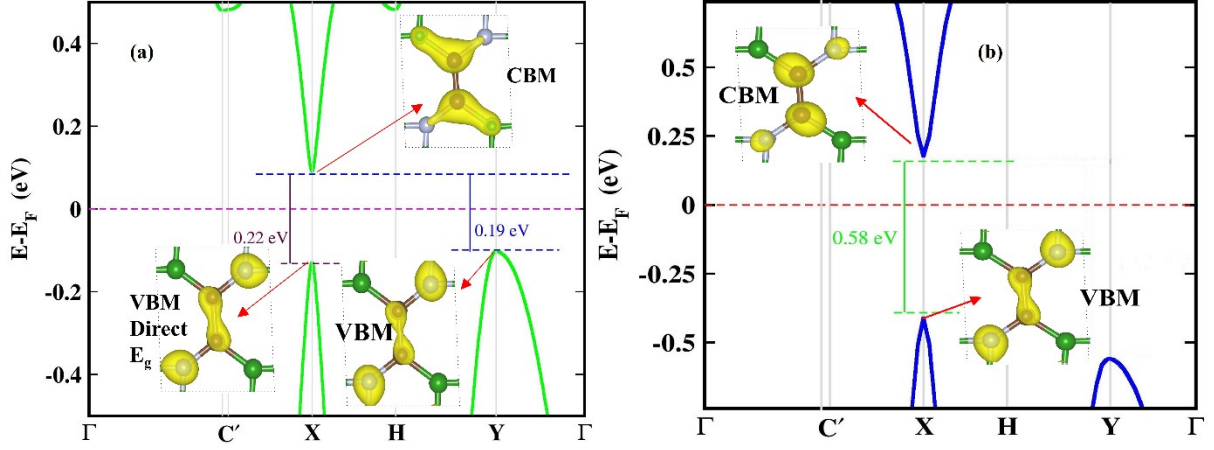


Fig. S7: VBM and CBM points along with wavefunction plots at iso-surface of $e/\text{\AA}ng^3$ using (a) GGA-PBE and (b) HSE functional.

Table S2: Calculated L values at different temperature for a particular value of doping for both n -type and p -type ($\mu - E_F = 0.1 \text{ eV}$).

T (K)	n-type			p-type		
	$\sigma \times 10^5$ ($S\text{m}^{-1}$)	κ_e ($\text{Wm}^{-1}\text{K}^{-1}$)	$L \times 10^{-8}$ ($\text{WS}^{-1}\text{K}^{-2}$)	$\sigma \times 10^5$ ($S\text{m}^{-1}$)	κ_e ($\text{Wm}^{-1}\text{K}^{-1}$)	$L \times 10^{-8}$ ($\text{WS}^{-1}\text{K}^{-2}$)
250	1.392	0.84	2.413	2.470	1.520	2.453
500	2.864	3.23	2.255	2.554	3.129	2.450
750	3.901	6.56	2.242	2.748	5.048	2.449
1000	5.537	12.01	2.169	3.375	8.263	2.448

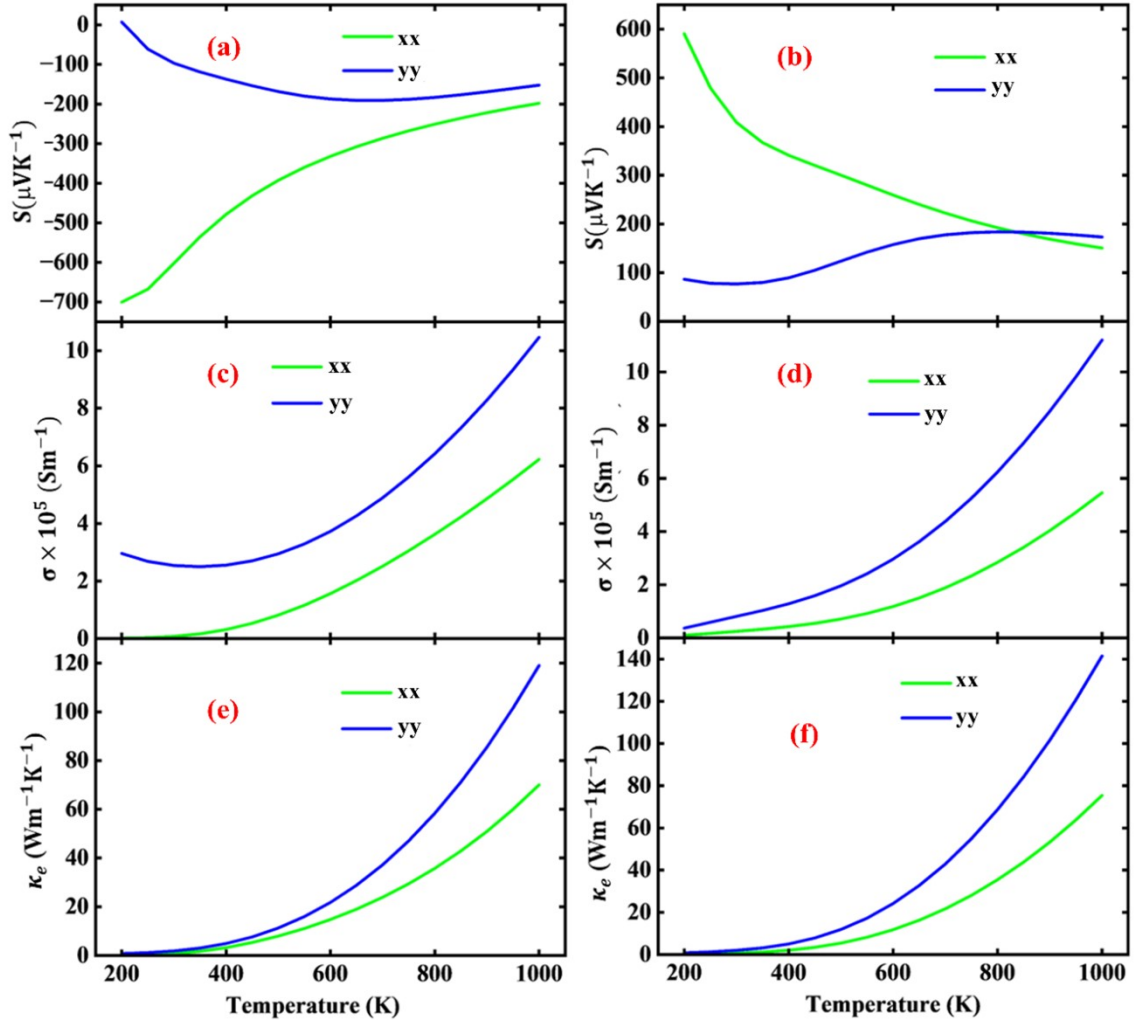


Fig. S8: Temperature-dependent variations of Seebeck coefficient (a, b), electrical conductivity (c, d), and electronic thermal conductivity (e, f) for (p-type, n-type) bpn-BCN monolayer.

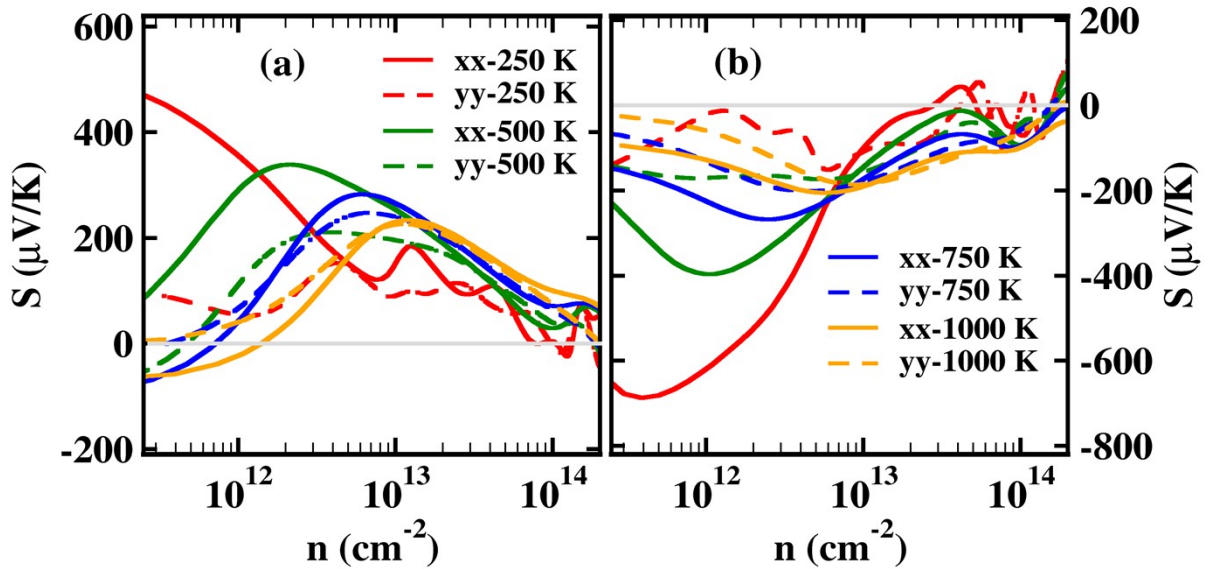


Fig. S9: Seebeck coefficients as a function of carrier concentration at different temperatures for (a) p-type doping and (b) n-type doping.

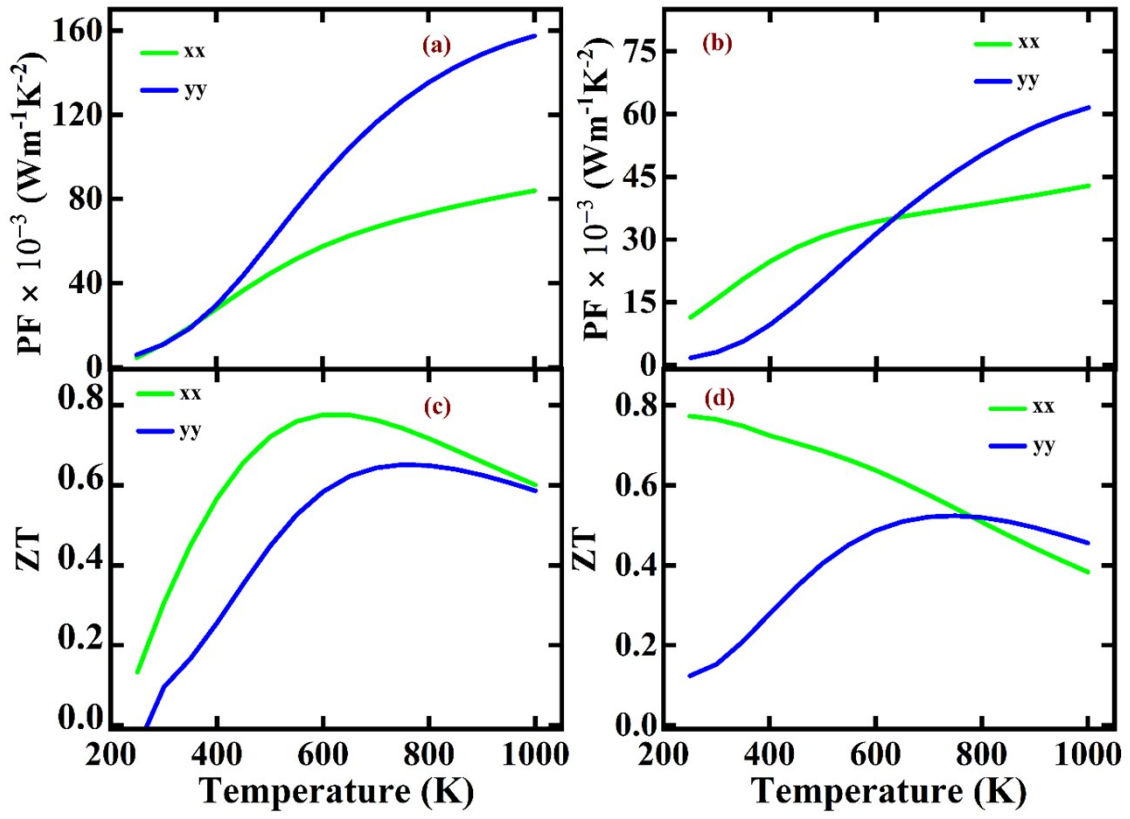


Fig. S10: (a) and (b) power factor and (c) and (d) figure of merit for p-type and n-type bpn-BCN monolayer, respectively.